Measurement of Thermal Properties of Polyaniline/Metal from Room Temperature to 170°C

G. P. Joshi,[1] N. S. Saxena,[1] T. P. Sharma,[1] S. Verma,[2] V. Dixit,[2] S. C. K. Mishra[2]

[1]*Condensed Matter Physics Laboratory, Department of Physics, University of Rajasthan, 5–6 Vigyan Bhawan, Jaipur 302 004, India*
[2]*National Physical Laboratory, Dr. K. S. Krishnan Road, New Delhi 110012, India*

Received 6 September 2002; accepted 18 December 2002

ABSTRACT: The heat transfer through polyaniline (PANI) mixed with metals (manganese and iron) is studied by measuring its effective thermal conductivity (λ_e) and effective thermal diffusivity (χ_e) from room temperature to 170°C at normal pressure. Simultaneous measurements of the λ_e and χ_e values of samples A (100% Fe), B (50% Fe and 50% Mn), and C (100% Mn) of the PANI mixtures with different percentages of Fe and Mn are carried out using the transient plane source technique. It is observed that the λ_e and χ_e of the above samples are almost independent of the temperature in a range of temperatures. However, maximum values for the λ_e and χ_e are found for sample A at ~140°C, sample B at ~130°C, and sample C at ~120°C. An empirical relationship deduced from a polynomial fit of the experimental data is established for the temperature dependence of the λ_e and χ_e values of these samples. Reasonably good agreement is obtained between the theoretically predicted results and the experimental data. This behavior is explained on the basis of bond formation between the metals (Fe and Mn) and nitrogen of the PANI matrix. © 2003 Wiley Periodicals, Inc. J Appl Polym Sci 90: 430–435, 2003

Key words: conducting polymers; mixing; thermal properties

INTRODUCTION

Conducting polymers have recently attracted a great deal of attention because of their many applications in light-weight batteries, solar cells, electrochromic switching, variable transmission windows, sensors, and nonlinear optical materials.[1] High conductivities are attainable when conducting polymers are doped with metals. Within the group of conducting polymer materials, there has been much interest in polyaniline (PANI), the most versatile of the conjugated polymers, because of its excellent stability under ambient conditions. In addition, a wide range of optical, electrical, and electrochemical properties make PANI an attractive material for a number of applications such as in displays, biosensors, and batteries. The PANI system possesses many unusual and attractive chemical aspects, including dopability by both oxidation and derivatization with a wide variety of substituents. These features and others play an increasingly important role in studies aimed at understanding the transport, magnetic, and optical properties of PANI.[2,3]

The basic chain structure in PANI exists in three insulating states: leucoemeraldine base (LB), emeraldine base (EB), and pernigraniline base. The energy gaps in LB and EB originate from the electronic structure of the backbone C_6H_4 units. The gaps in LB and EB rule out a bond alternation defect description of the charge states of PANI materials. Significant consequences of the ring-rotational degrees of freedom exist for the electronic structure and defect states of PANI.[4,5] The chemical formula of PANI is $[(\text{—B—NH—B—NH—})_Y(\text{—B—N=Q=N—})_{1-Y}]_X$, in which B and Q denote the C_6H_4 rings in the benzenoid and quinoid forms, respectively. When EB is equilibrated in a large excess of aqueous acid solution, protonation occurs at the imine repeat unit to produce the emeraldine salt of PANI (PA-ES), which is believed to have the following composition:

$$[(C_6H_4\text{—NH—}C_6H_4\text{—NH})_Y\text{—}(C_6H_4\text{—}\overset{+}{\underset{|}{N}}\underset{A^-}{}\text{H—}C_6H_4\text{=}\overset{+}{\underset{|}{N}}\underset{A^-}{}\text{H})_{1-Y}]_X$$

where A^- is the anion and it consists of equal numbers of reduced $[C_6H_4\text{—NH—}C_6H_4\text{—NH}]$ and $[C_6H_4\text{—N=}C_6H_4\text{=N—}]$ repeat units. This results in increased thermal and electrical conductivity. However, conductivity is affected by the protonation, level of oxidation, moisture contact, and polymerization conduction.

To improve the mechanical properties of PANI, metals are doped into it. PANI can achieve its highly

Correspondence to: N. S. Saxena (n_s_saxena@hotmail.com).

Journal of Applied Polymer Science, Vol. 90, 430–435 (2003)

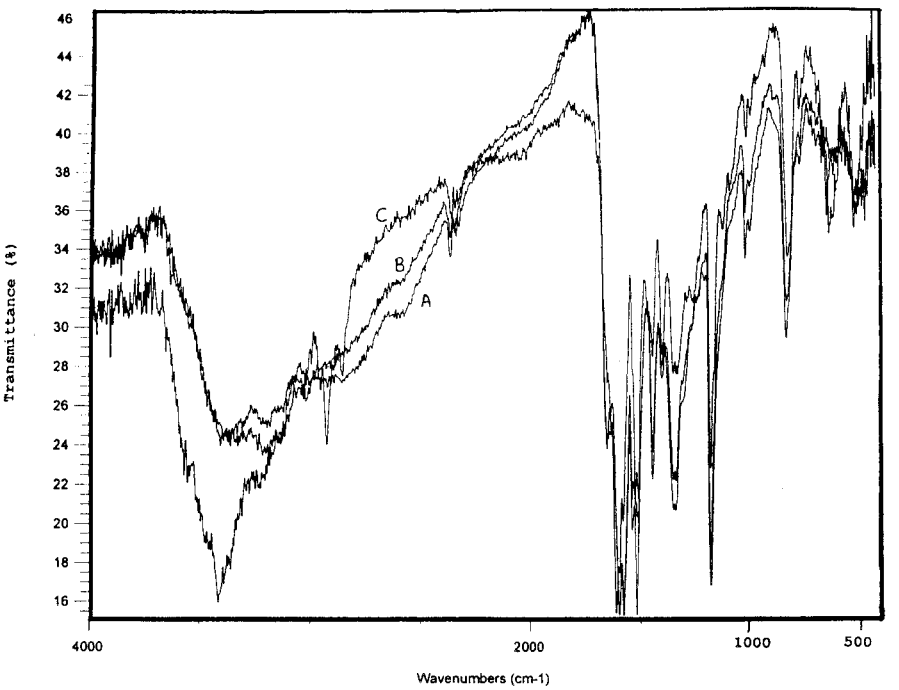

Figure 1 The FTIR spectra of samples A–C.

conductive state either through the protonation of the imine nitrogens (═N—) in its emeraldine state or through the oxidation of the amine nitrogens (—NH—) in its fully reduced leucoemeraldine state. Because X-ray photoelectron spectroscopy quantitatively determines the proportions of quinoid imine, benzenoid amine, and positively charged nitrogen in PANI, many researchers[6–8] have reported protonation by this method. The positively charged nitrogen portion is related to the doping level; in other words, the protonation level of the blends plays an important role in the thermal, as well as electrical, conduction of these materials.[9] Thus, the present study is aimed at studying the variation in these thermal properties of PANI mixed with metals (manganese and iron) over a temperature range of 30–170°C at normal pressure using the transient plane source (TPS) technique.

EXPERIMENTAL

PANI is usually prepared by redox polymerization of aniline using ammonium perdisulfate [$(NH_4)_2S_2O_8$] as an oxidant. Distilled aniline (0.02*M*) is dissolved in 300 mL of precooled HCl (1.0*M*) solution maintained at 0.5°C. A calculated amount of ammonium perdisulfate (0.05*M*) dissolved in 200 mL of HCl (1*M*) precooled to 0.5°C is added to the above solution. The dark green precipitate resulting from this reaction is washed with HCl (1.0*M*) untll the green color disappears. This precipitate is further extracted with tetrahydrofuran and *N*-methyl pyrolidinone solution by Soxhlet extraction and dried to yield the emeraldine salt. The EB can be obtained by heating the emeraldine salt with ammonia solution. A solution of metal halide is simultaneously prepared in distilled water. The solution is then slowly added to the precooled polymer solution with constant stirring. This composite is then dried in an oven at high temperature to attain the conducting polymer in powder form. The powder thus obtained can be used for device fabrication.

As a typical preparation, sample A (100% Fe) was synthesized by treating the aqueous solution of aniline, hydrochloric acid, and Fe taken according to the stoichiometry. The resulting solution was stirred thoroughly and added to the solution of alkali. The precipitated composite was washed repeatedly with distilled water till the filtrate was free of alkali (pH 7.5) and then dried in air. Similarly, sample B (50% Fe and 50% Mn) and sample C (0% Fe and 100% Mn) were synthesized using the same procedure but varying the quantities of Fe and Mn according to the stoichiometry. Figure 1 shows the Fourier transform IR spectroscopy (FTIR) spectra of samples A, B, and C. Formation of metal oxides and bonding between nitrogen and Fe or Mn is observed through the peaks in the spectrum of these samples in the range of 650–425 cm^{-1}. Pellets (2-mm thickness, 12-mm diameter) were prepared from the powdered materials with a pressure of 4.33 $\times 10^8$ Pa. The sample holder (Fig. 2) containing these samples is placed in a furnace that has a sensitivity of 1 K. After achieving isothermal conditions in the sample, a constant current pulse is passed through the heating element. The measurements reported in this article were performed with a TPS element of the type

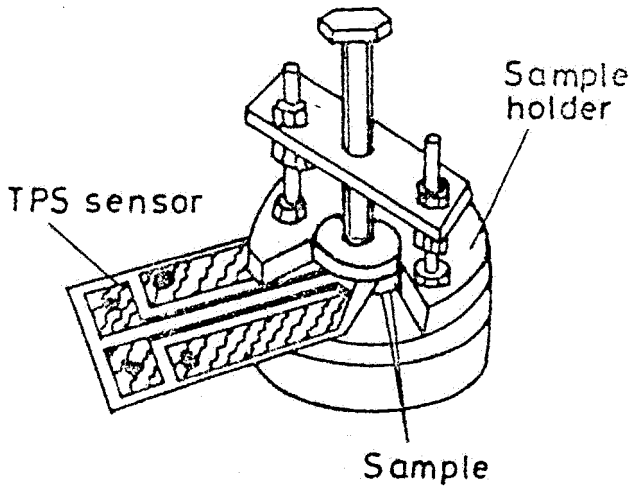

Figure 2 A schematic of the sample holder.

shown in Figure 3. It is made of 10 μm thick nickel foil with an insulating layer made of 50 μm thick kapton on each side of the metal pattern. The evaluation of these measurements was performed as outlined by Gustafsson.[10] No influence was recorded from the electrical connections, which are shown in Figure 4. These connecting leads had the same thickness as the metal pattern of the TPS element. Each TPS element had a resistance at room temperature of about 3.26 ω and a temperature coefficient of resistance (TCR) of around 4.6×10^{-3} K^{-1}. Because of the change in the average temperature of the sensor, the potential difference across it changes. The transient potential difference across the terminals is recorded by a digital multimeter, and the current through the TPS sensor is supplied by a digital power supply. The current in the circuit is adjusted according to the nature of the sample material. Multiple readings at appropriate intervals are taken to ensure the accuracy of the results. The TPS program used here is capable of recording the temperature of the sample through the TPS sensor itself. In addition, a sensitive thermometer is kept just above the sample pieces inside the furnace to monitor the temperature of the sample.

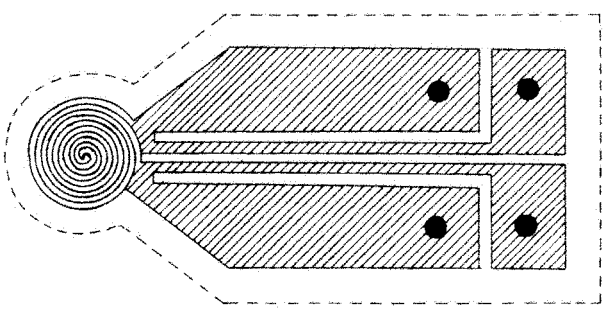

Figure 3 A schematic diagram of a transient plane source (TPS) sensor.

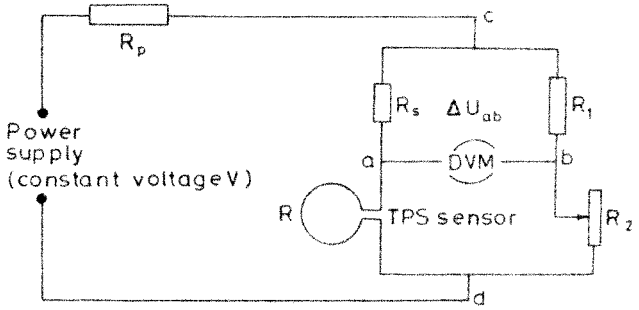

Figure 4 A schematic diagram of the electrical circuit for simultaneous measurements of the effective thermal conductivity and effective thermal diffusivity.

TPS theory

The TPS method consists of an electrically conducting pattern (Fig. 3) in the form of a bifilar spiral, which also serves as a sensor of the temperature increase in the sample. The sensor is sandwiched between the thin insulating layers of kapton. Assuming the conductive pattern to be in the y–z plane of a coordinate system inside the sample, the rise in the temperature at a point y, z at time t due to an output power per unit area Q is given by[10]

$$\Delta T(y,z,\tau) = \frac{1}{4\pi^{3/2}a\lambda}\int_0^{\tau}\frac{d\sigma}{\sigma^2}\int_A dy'dz'Q \left(y',z',t-\frac{\sigma^2a^2}{\chi}\right)\exp\left[\frac{-(y-y')^2-(z-z')^2}{4\sigma^2a^2}\right] \quad (1)$$

where $\chi(t - t') = \sigma^2a^2$, $\theta = a^2/\chi$, and $\tau = [t/\theta]^{1/2}$; a is the radius of the hot disk, which gives a measurement of the overall size of resistive pattern; θ is known as the characteristic time; σ is a constant variable; λ is the thermal conductivity (W/m K); and χ is the thermal diffusivity (m^2/s) of the sample material. The temperature increase ΔT (y, z, τ) attributable to a flow of current through the sensor gives rise to a change in the electrical resistance $\Delta R(t)$, which is given as

$$\Delta R(t) = \alpha R_0\overline{\Delta T(\tau)} \quad (2)$$

where R_0 is the resistance of the TPS element before the transient recording has been initiated, α is the TCR, and $\overline{\Delta T(\tau)}$ is the properly calculated mean value of the time-dependent temperature increase of the TPS element. During the transient event, $\overline{\Delta T(\tau)}$ can be considered to be a function of time only, whereas it will generally depend on such parameters as the output power in the TPS element, the design parameters[11] of the resistive pattern, and the thermal conductivity and thermal diffusivity of the surroundings. The value of $\overline{\Delta T(\tau)}$ is calculated by averaging the increase in temperature of the TPS element over the sampling time

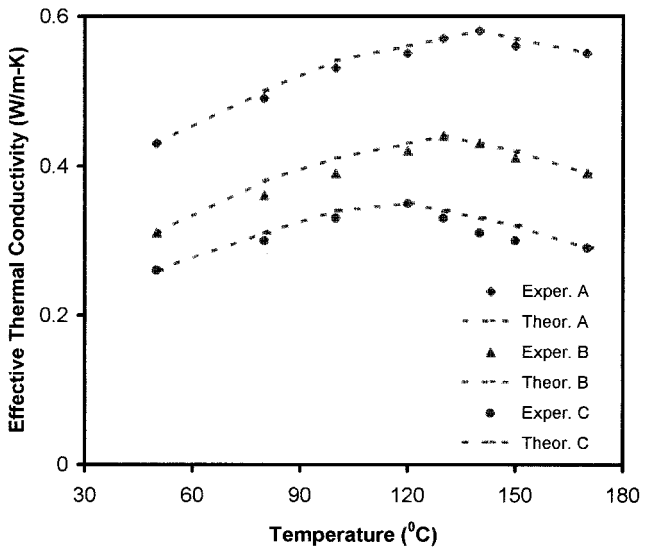

Figure 5 The temperature variation of the theoretical and experimental values of the effective thermal conductivity of samples A–C.

because the concentric ring sources in the TPS element have different radii and are at different temperatures during the transient recording.

It is possible to write down an exact solution[10] for the hot disk if it is assumed that the disk contains a number m of concentric rings as sources. From the ring source solution[12] we immediately get

$$\Delta T(\tau) = \frac{P_0}{\pi^{3/2} a \lambda} D_s(\tau) \tag{3}$$

where

$$D_s(\tau) = [m(m+1)]^{-2} \int_0^{\tau} \frac{d\sigma}{\sigma^2} \left[\sum_{l=1}^{m} 1 \left\{ \sum_{k=1}^{m} k \exp \frac{-(l^2+k^2)}{4\sigma^2 m^2} L_0\left(\frac{lk}{2\sigma^2 m^2}\right) \right\} \right] \tag{4}$$

where P_0 is the total output power, L_0 is the modified Bessel function, and l and k are the dimensions of the resistive pattern. To record the potential difference variations, which normally are of the order of a few millivolts during the transient recording, a simple bridge arrangement as shown in Figure 4 has been used. If we assume that the resistance increase will cause a potential difference variation $\Delta U(t)$ measured by the voltmeter in the bridge, the analysis of the bridge indicates that

$$\Delta E(t) = \frac{R_s}{R_s + R_0} I_0 \Delta R(t) = \frac{R_s}{(R_s + R_0)} \frac{I_0 \alpha R_0 P_0}{\pi^{3/2} a \lambda} D_s(\tau) \tag{5}$$

where

$$\Delta E(t) = \Delta U(t)[1 - C\Delta U(t)]^{-1} \tag{6}$$

and

$$C = \frac{1}{R_s I_0 \left[1 + \dfrac{\gamma R_0}{\gamma(R_s + R_0) + R_p} \right]} \tag{7}$$

The various resistances are found in Figure 4, where R_p is the lead resistance; R_s is a standard resistance with a current rating that is much higher than I_0, which is the initial heating current through the arm of the bridge containing the TPS element; and γ is the ratio of the resistances in two ratio arms of the bridge circuit, which is taken to be 100 in the present case.

RESULTS AND DISCUSSION

Many investigators have observed the effect of dopants on the physical properties of conducting polymers in electrical, optical, and differential thermal analyses. In this article the variation of the effective thermal conductivity (λ_e) and effective thermal diffusivity (χ_e) of the PANI sample mix with Fe and Mn has been studied from room temperature to 170°C using the TPS method. The variation of these two thermal properties with temperature is shown in Figures 5 and 6. Figure 5 shows the variation of the effective thermal conductivity with temperature of all the conducting polymers mixed with Fe and Mn in different percentages. Figure 6 shows the variation of the effective thermal diffusivity with temperature. Note that the λ_e and χ_e of each sample increase to a maximum and then

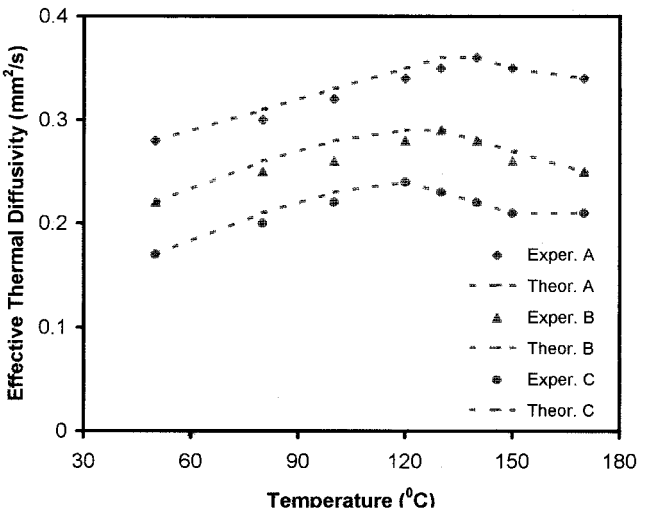

Figure 6 The temperature variation of the theoretical and experimental values of the effective thermal diffusivity of samples A–C.

decrease with a further increase of temperature beyond a characteristic temperature, which varies for different samples. It has been seen that the effective thermal conductivity of the composite of PANI mixed with Fe (100%) increases with temperature initially and attains a maximum at around 140°C for sample A. The maximum value of the effective thermal conductivity for sample A is 0.58 W/m K. When the temperature is increased beyond 140°C, the value of the effective thermal conductivity starts decreasing. With the decrease of the concentration of iron (50% Fe) and the increase of the concentration of manganese (50% Mn), the peak values of the effective thermal conductivity and effective thermal diffusivity are shifted to 130°C. Thus, the increase in the crosslinking density of sample B results in the decrease of the effective thermal conductivity and effective thermal diffusivity. In addition, with the increase of the concentration of Mn (100%), the peak values of the effective thermal conductivity and effective thermal diffusivity are shifted to 120°C, which is also an indication of less strong bond formation between nitrogen and Mn. It is interesting to note that the bonding between the nitrogen and Mn of the Mn-rich PANI mix is less strong and loose as compared to the bonding of the nitrogen and Fe of the Fe-rich PANI mix because of the more stable electronic configuration of Mn as compared to Fe. In all the samples, the effective thermal conductivity and effective thermal diffusivity increase with increasing temperatures and show a similar tendency, regardless of the PANI content. In addition, the effective thermal conductivity and effective thermal diffusivity in all samples slowly decrease beyond the characteristic temperature (ranging between 120 and 140°C).

Conducting polymers can be polycrystalline or amorphous in nature and may belong to inorganic, organic, or combinations of inorganic and organic classes of materials. These samples are prepared at low temperature by the sol–gel technique, which upon heating at high temperature gives rise to single phase crystalline or multiphasic crystalline ceramics. In the temperature region before and after the peak in the thermal conductivity versus temperature curve, structure scattering, which is independent of temperature, plays an important role in the thermal resistance. The observed variation in the thermal conductivity is explained on the basis of various phonon scattering mechanisms,[13–15] namely, structural scattering, stray scattering, and chain defect scattering. First, PANI is not charge conjugation symmetric because neither the Fermi level nor the band gap are formed in the center of the π band, thus making the valence and conduction bands asymmetric. Second, both carbon rings and nitrogen atoms are within the conjugation path, forming a generalized A–B polymer. Third, EB forms an insulating metallic state if protons are added to the —N═ sites while the number of electrons in the chain is held constant. The experimental values of the effective thermal conductivity and effective thermal diffusivity at room temperature for samples A, B, and C are given in Table I. It is observed that at room temperature the values of the effective thermal conductivity and effective thermal diffusivity decrease with the increase of Mn content in the PANI matrix (i.e., $\lambda_A > \lambda_B > \lambda_C$ and $\chi_A > \chi_B > \chi_C$). For a further increase of the temperature over the characteristic temperature T_0 (where λ_e and χ_e show their maxima), the effective thermal conductivity and thermal diffusivity decrease very slowly. In addition, the thermal conductivity of Fe at room temperature is greater than the thermal conductivity of Mn. The electronic configurations of Fe ($z = 26$) and Mn ($z = 25$) are $[Ar]3d^64s^2$ and $[Ar]3d^54s^2$, respectively. In the PANI matrix the nitrogen has one pair and, when metal is doped in the matrix, bond formation between the metal (Fe and Mn) and nitrogen takes place. This bond formation is responsible for the thermal stability of the mix. A further addition of Mn in the PANI matrix decreases this stability and thereby the effective thermal conductivity and effective thermal diffusivity.

TABLE I
Values of Effective Thermal Conductivity and Diffusivity at Room Temperature for Samples A–C

Sample Code	Effective Thermal Conductivity (W/m K)	Effective Thermal Diffusivity (mm^2/s)
A (Fe = 100%)	0.39	0.25
B (Fe, Mn = 50%)	0.28	0.19
C (Mn = 100%)	0.24	0.15

Defects are always present at high temperatures. Imperfections occur in crystals as a result of dislocation of ions, ion vacancies in the lattice, a nonstoichiometric proportion of the ions present, or simply foreign ions or "impurities" in the lattice. A perfect metallic conductor should have zero resistance, because resistance arises from the scattering of electrons by lattice imperfections. Because of the thermal motions of the atoms as the temperature is raised, this scattering of electrons increases in concentration. Defect formation frequently leads to the development of semiconducting properties that rapidly increase with increases in temperature. The atoms in metals are joined by a special metallic bond. Metals have the tendency to lose electrons to form M^+ ions. The magnetic properties are given by the number of unpaired electrons in the nonbonding orbitals: Mn is paramagnetic and Fe is ferromagnetic. Because Fe has the maximum number of unpaired electrons in nonbonding orbitals, it has the most magnetic properties when doping in the PANI matrix creates a metallic bond. The bond strength between nitrogen and iron is improved, and it is also correlated with the thermal properties.

By means of a least squares fit to the experimental data of λ_e and χ_e as a function of temperature, as plotted in Figures 5 and 6 for samples A–C, empirical relationships have been established for the theoretical prediction of λ_e and χ_e. These are given as

$$\lambda_e = A + B(T - T_0)^2 + C(T - T_0)^3 \quad (8)$$

$$\chi_e = a + b(T - T_0)^2 + c(T - T_0)^3 \quad (9)$$

where A, B, C, a, b, and c are constants calculated by experimental conditions and T is the temperature of the composite in absolute temperature units. The observed variations in λ_e and χ_e with temperature can be explained by considering the effect of temperature on structural units in a phenomenological manner. In the temperature range below T_0 the temperature dependence of λ_e and χ_e is controlled by the variation of the phonon mean free path due to structure scattering, stray scattering, and chain defect scattering. The first terms A and a in both empirical equations represent the contribution to the thermal resistance of structure scattering. For temperatures below T_0, the structure scattering becomes predominant, in addition to chain defect scattering, scattering due to defects introduced by blends, and the relatively smaller length of the chain segments. With rising temperature the polymeric chain straightens out more and more. Therefore, the mean free path increases and thus the contributions to the corresponding thermal resistance decreases linearly with the rise of temperature, resulting in the increase of λ_e and χ_e in this temperature range. The chain defects are effectively identical to stacking faults and hence are expected to show similar temperature dependence for thermal resistance. The constant B in eq. (8) represents the thermal resistance by chain defect scattering. The constant C can also be attributed to the contribution to thermal resistance by other possible stray scattering mechanisms. Constants A, B, C, a, b, and c are conducting polymer dependent parameters. This means that they should change systematically with the Mn and Fe contents in the PANI matrix, and the obtained value of these constants supports this dependence as shown in Tables II and III. Figures 5 and 6 also show the variation of λ_e and χ_e with temperature as predicted by empirical relations (8) and (9) for samples A–C. It is clear from Figures 5 and 6 that the agreement is very good between the predicted values of λ_e and χ_e using the empirical relation and the results of the experiment.

TABLE II
Value of Constants A, B, and C in Eq. (8) for Effective Thermal Conductivity for Samples A–C

Sample Code	Peak Temp. Value (°C)	Constant for Effective Thermal Conductivity of Samples A–C		
		A (W/m K)	Ba (W/m K^3)	C (W/m k^4)
A (Fe = 100%)	140	0.58	-2.9×10^{-5}	-1.2×10^{-7}
B (Fe, Mn = 50%)	130	0.44	-2.8×10^{-5}	-9.1×10^{-8}
C (Mn = 100%)	120	0.35	-2.2×10^{-5}	-4.7×10^{-8}

TABLE III
Value of Constants *a*, *b*, and *c* in Eq. (9) for Effective Thermal Diffusivity for Samples A–C

Sample Code	Peak Temp. Value (°C)	Constant for Effective Thermal Diffusivity of Samples A–C		
		a (mm^2/s)	*b* (mm^2/s K^2)	*c* (mm^2/s k^3)
A (Fe = 100%)	140	0.36	-1.9×10^{-5}	-1.0×10^{-7}
B (Fe, Mn = 50%)	130	0.29	-2.1×10^{-5}	-1.2×10^{-7}
C (Mn = 100%)	120	0.24	-1.2×10^{-5}	$+1.9 \times 10^{-8}$

CONCLUSIONS

Study of the variations of the effective thermal conductivity and effective thermal diffusivity of PANI doped with Fe and Mn with temperature is suggestive of the fact that the characteristic temperature and stability is increased with the increase of the concentration of higher conducting metals into PANI. This is attributable to the increase in crosslinking density of PANI mixed with Fe as compared to PANI mixed with Mn.

References

1. Fried, J. R. Polymer Science and Technology; Prentice Hall India Ltd.: New Delhi, 1999.
2. Ram, M. K.; Mehrotra, R.; Pandey, S. S.; Malhotra, B. D. Phys Condens Mater 1994, 6, 8913.
3. Sariciftci, N. S.; Smilowitz, L.; Cao, Y.; Heeger, A. J. Synth Met 1993, 55, 188.
4. Ginder, J. M.; Epstein, A. J. Synth Met 1990, 37, 45.
5. Sauvajol, J. L.; Djurado, D.; Dianoux, A. J.; Fischer, J. E.; Scherr, E. M.; Macdiarmid, A. G. Phys Rev B 1993, 47, 9.
6. Yue, J.; Epstein, A. J. Macromolecules 1991, 24, 4441.
7. Li, Z. F.; Kang, E. T.; Neoh, K. G.; Tan, K. L. Synth Met 1997, 87, 45.
8. Umare, S. S.; Borkar, A. D.; Gupta, M. C. 2002, 25, 235.
9. Han, M. G.; Im, S. S. Polymer 2000, 41, 3253.
10. Gustafsson, S. E. Rev Sci Instrum 1991, 62, 797.
11. Gustafsson, S. E.; Suleiman, B.; Saxena, N. S.; Haq, I. U. High Temp High Press 1991, 23, 289.
12. Carslaw, H. S.; Jeger, J. C. Conduction of Heat in Solids; Oxford University Press: New York, 1959.
13. Dhami, A. K.; Dey, T. K. Bull Mater Sci 2000, 23, 439.
14. Saxena, N. S.; Pradeep, P.; Mathew, G.; Thomas, S.; Gustafsson, M.; Gustafsson, S. E. Eur Polym J 1999, 35, 1687.
15. Dashora, P.; Saxena, N. S.; Saksena, M. P.; Sharma, K. B.; Sachdev, K.; Pradhan, P. R.; Ladiwala, G. D. Phys Scripta 1992, 45, 399.